Detection and size estimation of crack in plate based on guided wave propagation

Beata Zima *, Rafał Kędra

Department of Mechanics of Materials and Structures, Faculty of Civil and Environmental Engineering, Gdańsk University of Technology, ul. Narutowicza 11/12, 80-233 Gdańsk, Poland

A R T I C L E   I N F O

A B S T R A C T

The paper presents results of the comprehensive theoretical and experimental investigation of crack detection in metallic plate using guided wave propagation. The main aim of the paper is to develop the novel method which would allow for linear crack size estimation with the use of minimal number of the transducers. In general, there exists the relation between length of the propagation path and the wave amplitude value. However, we have shown that the amplitude value can be also influenced by the interaction with the damage. The meaningful differences in the amplitudes of waves reflected from various damage zones (the end and middle point) have become the foundation of the novel algorithm of line-crack detection. All stages of the algorithm have been described in detail and then the experimental tests were conducted. The experimental investigation involved crack detection and its size estimation for four different configurations of piezo transducers. Each configuration consisted of one actuator and three sensors, what which so far was the minimum number of sensors for point damage detection. The damage maps created on the basis of the collected time-domain signals visualized the exact crack orientation in each case. It has been revealed that the developed algorithm allows also for determining the crack size when the configuration of the transducers is designed properly.

© 2020 The Author(s). Published by Elsevier Ltd. This is an open access article under the CC BY-NC-ND license (http://creativecommons.org/licenses/by-nc-nd/4.0/).

1. Introduction

In general, guided waves, because of their ability to travel relatively long distances without the significant loss of energy, are a suitable tool in non-destructive damage detection in various engineering structures. The great potential of the use of waves in Structural Health Monitoring (SHM) has been proven in the recent decades by many scientists [1–4]. The long propagation range of guided waves allowing for fast-screening large areas has been particularly useful in plate-like structures diagnostics. Works on improving the methods of damage detection in plate-like structures has been carried out for last years in many different directions. The crack orientation in plate structure and its influence on wave amplitude was considered by Tua *et al.* [5]. They monitored the peak energy due to reflection from variably oriented damage. Various configurations consist of nine transducers and their effectiveness in point damage detection in plates were described by Wandowski *et al.* [6]. The use of guided waves in damage detection in a stiffened plate was investigated by Radzieński *et al.* [7]. Their damage identification method based on a laser scanning and RMS maps proved to be suitable for diagnostics of stiffened structural elements. Li *et al.* [8] investigated an influence of number of PZT transducers, steering angle and diameter of their array on the

---

* Corresponding author.
E-mail address: beata.zima@pg.edu.pl (B. Zima).

quantitative damage image construction for plate structures. The dynamic characteristics of Lamb waves in order to be used for material evaluation and damage inspection of thin-walled structures was investigated by Pai *et al.* [9]. Wang *et al.* [10] introduced a soft-thresholding method based on the discrete wavelet transform and the empirical mode decomposition for the Lamb wave-based damage identification in plate-like structures. Their approach was investigated numerically and experimentally with the use of a circular array of twelve sensors attached to cracked plate. A development of a fuzzy-logic system for delamination detection in composite plates with material and measurement uncertainty was presented by Chandrashekhar and Ganguli [[11]. Rectangular phased array of sixteen piezoelectric transducers was used by Liu *et al.* [12] for damage localization in aluminum plate. They adopted Total Focusing Method and Sign Coherence Factor images to improve clarity of damage maps. The problem of wave propagation in plates with step discontinuities was studied analytically and numerically by Schaal and Mal [13]. Their investigation proved that decaying of the incident antisymmetric and symmetric modes is related with increase of the step size. Ellipse-based damage detection algorithm for monitoring damage growth in steel plates was presented by Zima and Rucka [14]. They revealed that for given configuration of sensors there is a certain limit length of damage which can be detected. A circle based algorithm was used by Chen *et al.* [15] for localization and estimation the extent of damage in aluminum plate. They detected a punch hole and estimated its size by two different configurations of transducers. Micro-cracks in metallic plates by nonlinear wave propagation were detected by Jingpin *et al.* [16]. Zuo *et al.* [17] presented a novel model-based 2D multiple signal classification damage identification algorithm for plate structures. The array of seven transducers was used to detect two different damages in 16-layered, composite, anisotropic plate. Kim and Yuan [18] described an enhanced damage imaging algorithm using matching pursuit algorithm with multiple wavepaths. They used array of four sensors to visualize the point damage location in a metallic plate. In the paper [19] Kudela *et al.* proposed a novel approach of piezoelectric array steering for crack detection in plate. Its usefulness was proved by circular array of twelve sensors. Cantero-Chinchilla *et al.* [20] described a Bayesian methodology for damage location using guided waves. In their experiment fourteen and six sensors were used. Mori *et al.* [21] developed a damage detection method based on the time reversal focusing and the mode-converted Lamb wave without baseline data for non-symmetric defects in plates in the thickness direction. Sen *et al.* [22] proposed two sparsity based damage detection algorithms for plates using guided waves. Response profiles of the system for different locations of damage were constituted by a dictionary of damage characterization matrix.

Despite the significant number of papers about guided wave utilization in damage detection in plate-like structures, an exact damage size estimation is still a great challenge. Moreover, in the majority of the above reported works, a significant number of transducers had to be used to identify the location of the point small-size damage. It is well know that for unambiguous location of point damage, the configuration of at least three sensors needs to be used [6]. In the case of linear cracks or damages characterized by bigger size, it is necessary to attach more sensors, which significantly increases the number of registered signals and improve information about investigated object, but also rises the costs of the monitoring system and extends the analysis time. Therefore, from the point of view of remote, fast and efficient monitoring system, the number of attached transducers should as small as possible.

The main aim of the paper is to develop the method which would allow for the linear crack detection and its size estimation with the use of minimal number of the transducers. To this end, at the first stage a theoretical analysis was conducted regarding the influence of the propagation path length on wave amplitude. The analytical relationship between the distance from excitation source and the wave amplitude has been derived using Dispersion Compensation Method and verified experimentally. The comprehensive experimental study of wave interaction with a crack was conducted and it has been proven that the signal amplitude is significantly influenced not only by the length of the propagation path, but also by the crack zones (end point or middle point of the crack) from which wave is reflected. The meaningful differences in the amplitudes of waves reflected from the end and the middle point of the damage have been presented and have become the foundation of the novel algorithm of linear crack detection. All stages of the novel algorithm have been described in detail and then experimentally tested. The experimental investigation involved the crack detection and its size estimation by four different configurations of piezo transducers. Each configuration consisted of one actuator and three sensors, which so far was the minimum number of sensors required for point damage detection. The damage maps created on the basis of the collected time-domain signals visualized the exact crack orientation. It has been revealed that the developed algorithm allows also for the exact determining of the crack size when the configuration of the transducers is properly designed. The algorithm can be especially useful for constant monitoring of damages which are not dangerous enough to require immediate intervention and structure repairing, but it is necessary to observe their development, due to possible dangerous consequences in the future. The proposed method is quantitative, which means that it allows a reliable assessment of the risk of damage of failure of the entire structure. The paper discusses both advantages and disadvantages of the developed approach.

2. Relation between wave amplitude and length of the propagation path

In this section the relation between amplitude and the length of the propagated distance, which is an important prerequisite for the implementation of the new algorithm, is analyzed and discussed. Both types of results, analytical and experimental are presented and compared.

As the Lamb wave travels along plate its amplitude decays. According to the assumption of the constant signal energy, the amplitude decreases but wave packet spreads because of dispersion effect. The exponential decay of Lamb wave amplitude

was demonstrated by Ghadami et al. [23], Ramadas et al. [24], Rose [25] and many other researchers. The attenuation of Lamb waves can be in general described as follows [23]:

$$A_2 = A_1 e^{-k_i \Delta x}, \tag{1}$$

where A_1 and A_2 are the amplitudes registered at the distance Δx and k_i is attenuation coefficient which can be determined by the expression:

$$k_i = \frac{f \xi}{c_g}, \tag{2}$$

where f is the excitation frequency, c_g is wave group velocity and ξ is the structural damping. The relation between wave amplitude and the travelled distance was also proposed by Su and Ye [26]. They observed that the magnitude of Lamb wave is proportional to the inverse square root of the propagation distance:

$$\frac{A_1}{A_2} = \frac{\sqrt{d_2}}{\sqrt{d_1}}, \tag{3}$$

Despite that in literature we can find the relationships between the amplitude and distance traveled, predicting the amplitude value is often very difficult because of the necessity of an accurate structural damping determining. Moreover, the value of the amplitude registered by the PZT sensors is also affected by the manner and a quality of the bonding of the sensor, a type of wax or glue and its temperature. The work presented by Ramadas et al. [24] shows the comparison between experimental and numerical results of the investigation of wave attenuation with the distance however, their investigation involved relatively small distances from the excitation source.

The results presented in the further parts of this article concerns signals captured by the sensors located further from the excitation source. In addition, the presented method of the amplitude value determining based on Dispersion Compensation allows for reduction of the influence of imperfect bonding between the sensor and the structure.

2.1. Amplitude-distance relationship derivation using Dispersion Compensation method

We derive the relation between the amplitude and the traveled distance using Dispersion Compensation method (DCM). The DCM is a well-known and widely used approach [27,28], which allows to predict the time variability of the propagating waveform $u(x,t)$ at the known distance from the source based only on the excitation function and the angular frequency-wavenumber relationship $k(\omega)$. The fundamental DCM equation has the following form:

$$u(x, t) = \int_{-\infty}^{\infty} F(\omega) e^{j[\omega t - k(\omega)x]} d\omega, \tag{4}$$

where: $F(\omega)$ is the angular frequency variability of the excitation function and $\times$ is a spatial coordinate – distance from the wave source. In the case of the plate structures the angular frequency versus wavenumber dependency can be determined using Lamb-Rayleigh theory [29], by solving two dispersion equations for symmetric and antisymmetric modes:

$$\begin{aligned} \frac{\tan(qh)}{\tan(ph)} &= -\frac{4k^2 pq}{\left(k^2 - q^2\right)^2} \\ \frac{\tan(qh)}{\tan(ph)} &= -\frac{\left(k^2 - q^2\right)^2}{4k^2 pq}, \end{aligned} \tag{5}$$

In the above equations the parameters p and q are related with the wavenumber, angular frequency, longitudinal wave velocity (c_L) or shear wave velocity (c_T) as follows:

$$p^2 = \frac{\omega^2}{c_L^2} - k^2, \ q^2 = \frac{\omega^2}{c_T^2} - k^2. $$

A slight disadvantage of the using the Lamb-Rayleigh equations is that they are based on two-dimensional wave propagation problem in a plane-strain structure. As the result, they allow only for an accurate simulating the shape of the waveform, but do not provide the information about its amplitude. An additional parameter related to the propagation distance should be introduced to overcome these limitations. Let's assume that the source with the known time dependency f(t) of the wave is point-like, the disturbance spreads in all directions in the plate-like structure and there is no material damping. Because wave travels in all directions with the same velocity, the shape of the wavefront is circular. In such a case, there is no energy loss and the total energy measured on each circuit of the wavefront with a center at the excitation point is constant. If we know the time variation of the signal measured at a distance r from the excitation point $U(r,t)$, the total energy of the propagating wavefront can be described as:

$$E = \int_{-\infty}^{\infty} 2\pi r \, U(r,t)^2 dt = const, \tag{6}$$

For the same excitation function $f(t)$ the energy obtained using DCM and Lamb-Rayleigh theory for $x = r$ is equal to $\int_{-\infty}^{\infty} u(r,t)^2 dt$. Both values must be equal and, if we assume that DCM well simulates the shape of a wave packet, we can formulate the following equation:

$$2\pi r \, U(r,t)^2 = u(r,t)^2 \Rightarrow U(r,t) = \frac{u(r,t)}{\sqrt{2\pi r}}, \tag{7}$$

It means that in order to take into account the spatial propagation of the wave, the signal determined using DCM should be divided by the square root of the propagation distance multiplied by 2π. This knowledge is necessary for the correct modelling of the amplitude versus the propagation distance dependency. Furthermore, because the above considerations did not include energy loss due to material damping, an additional factor in the form of an exponential multiplier $e^{-r\xi}$ was added to Eq. (7) and finally it takes the following form:

$$U_d(x,t) = \frac{e^{-r\xi}}{\sqrt{2\pi r}} \int_{-\infty}^{\infty} F(\omega) e^{j[\omega t - k(\omega)x]} d\omega. \tag{8}$$

2.2. Experimental distance-amplitude curve

To determine the damping coefficient and to trace the experimental amplitude-distance relationship, the guided waves were propagated in the steel plate, which is also considered in the further parts of the experimental study. The plate dimensions were 125 cm × 125 cm × 0.1 cm. The material parameters of steel were as follows: the elastic modulus $E = 213$ GPa, the Poisson's ratio $v = 0.33$ and the density $\rho = 7780$ kg/m^3. In the first stage of the experimental investigation the sensor-actuator pair was attached to the plate surface near its edge (Fig. 1). The input function was a five-cycle sine with a central frequency 100 kHz modulated by the Hann window. In general, for each frequency at least two wave modes can be excited: symmetric and antisymmetric. Because the excitation was perpendicular to the plate surface in each investigated case, we took into account only antisymmetric modes. The sensor first registered the incident wave excited by an actuator and then captured the reflection from the edge of the plate. For the known lengths of the propagation paths L and assuming that the dissipation of wave energy during the reflection from the edge can be neglected, the ratio between amplitude values of incident and reflected wave could be used to assess the damping coefficient. Several different configurations of the transducers were used to collect enough data allowing for the precise tracing the distance-amplitude curve. Only four exemplary configurations are presented in Fig. 1. It can be seen that the subsequent configurations are selected so that the results can be referenced and normalized with respect to each other. In this way, the problem arising in the case of sensors connected to the structure by adhesive layer (e.g. by wax or glue), when the amplitude signal amplitude depends on the layer parameters was eliminated.

The next step was to fit the analytical distance-amplitude curve described by Eq. (8) based on experimentally obtained data. The calculations were carried out using authors' code written in MATLAB environment. The dispersion Lamb-Rayleigh (Eq. (5)) was solved in a discrete form using a trapezoidal numerical integration for the frequency increment $\Delta\omega = 12.07 \cdot 10^3$ rad/s. For this frequency value the convergence of experimental and theoretical results was obtained – the lower value would involve a longer time. The damping coefficient was determined by the systematic search method and it was set as
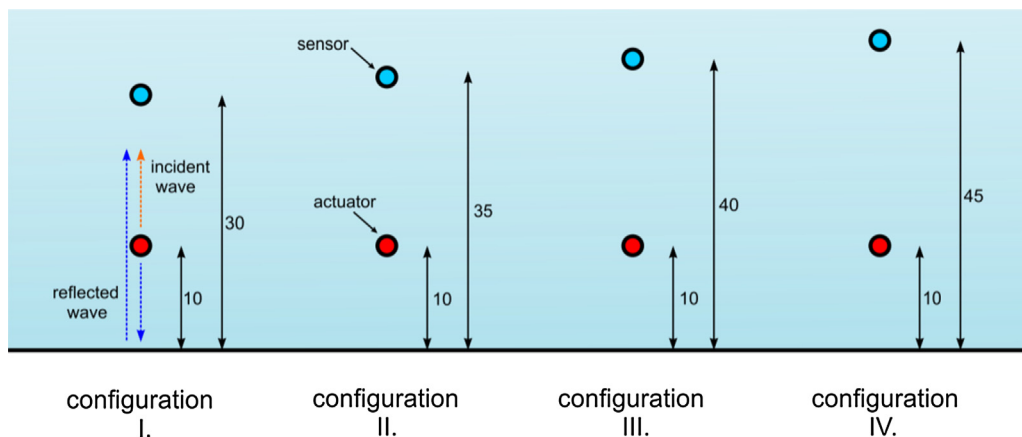

Fig. 1. Configurations of actuator-sensor pair for determining the damping coefficient.

ξ = 0.335. The results were normalized to the amplitude of signal measured 0.6 m from the source. To determine the amplitudes' values of the wave packets, the envelopes of the signals were created using the Hilbert transformation.

Fig. 2a shows the final results of the dispersion simulation using Eq. (8). Fig. 2b includes also intermediate results. It can be see that the data obtained by the direct using of DCM, according to Eq. (4) plotted by a green, solid line are not comparable with experimental results denoted by the black dots. Introducing the additional factors in the form of square root from $2\pi r$ and $e^{-r\xi}$ has significantly improved results quality. The determination coefficient was equal R2 = 0.898 in the case of using only one fist one ($\sqrt{2\pi r}$) and using both ($\sqrt{2\pi r}$ and $e^{-r\xi}$) it reached the value R2 = 0. 982. The high value of the determination coefficient confirms the correctness of the adopted methodology for determining the relationship between amplitude and length of the propagation path.

In practice, the obtained distance-amplitude dependence can be used in two different ways. First, for the known length of the propagation path the amplitude of wave packet can be predicted. Secondly, the length of the propagation path can be determined on the basis of the amplitude without any information about time of flight (ToF) or wave velocity.

2.3. Wave reflection from various damage zones

At the second stage of the experimental investigation the reflections from various damage zones (middle and end points) have been studied. The main aim of this part of investigation was to analyze the influence of the place, where wave reflects on the signal amplitude.

The schematic visualizations of wave reflection from the damage presented in Fig. 3 were performed in Abaqus environment. In general, when wave reflects from the straight edge of the crack (Fig. 3a), the shape of the reflected wavefront is different than in the case of wave reflection from the end of the crack (Fig. 3b). When wave reflects from the middle part of the line crack, the radiuses of the reflection and propagating wavefront are the same and they are equal to r_1 (Fig. 3a). It is noteworthy that the radius r_1 can be also interpreted as the length of the propagation path r occurring in the Eqs. (6)–(8).

When wave reflects from the end point of the crack (Fig. 3b), the radius of the reflected wavefront denoted as r_3 is different (smaller) than radius of the primary wavefront r_2. In such a case we cannot speak about the equality of the propagation path length ($r_2 = r$) and the radius of the reflected wavefront r_3. As a consequence, amplitude of the reflection cannot be easily determined with the use of Eq. (8).To verify the theoretical predictions and to investigate the influence of the place of reflection on the amplitude, six different configurations of actuator and sensor were involved and propagation signals containing the reflections from the crack were collected during experimental tests (Fig. 4). The length of the propagation path actuator–damage–sensor can be easily theoretically determined on the basis of the Fermat's principle also known as the principle of the least time. Fermat's principle says that out of all possible paths that wave ray can take between two points, it takes the path which requires the shortest time [30]. On the basis of this principle for the known actuator and sensor locations, the place where the wave reflects from the damage can be accurately indicated. In the three cases (configurations I, II and III) the shortest path assumed that wave is reflected from the middle part of the damage. In the next three cases (configurations IV, V and VI) wave was reflected from the damage end point.
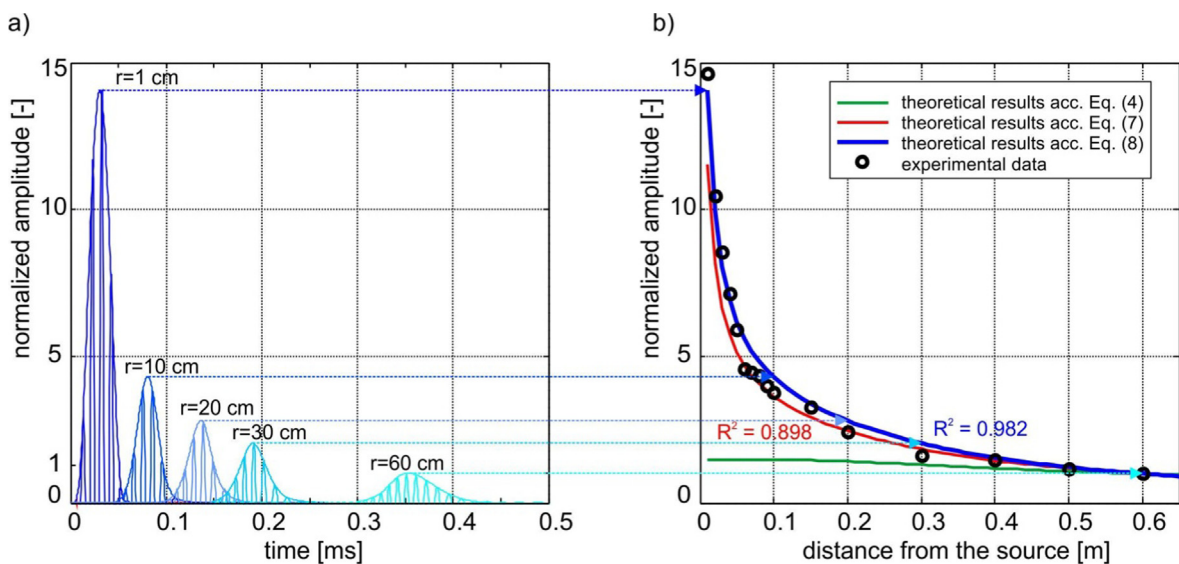

Fig. 2. Results on Dispersion Compensation Method simulation (a) and Distance-amplitude curve (b) determined for steel plate investigated in experiment (○– experimental results, ▬ fitted analytical curves).
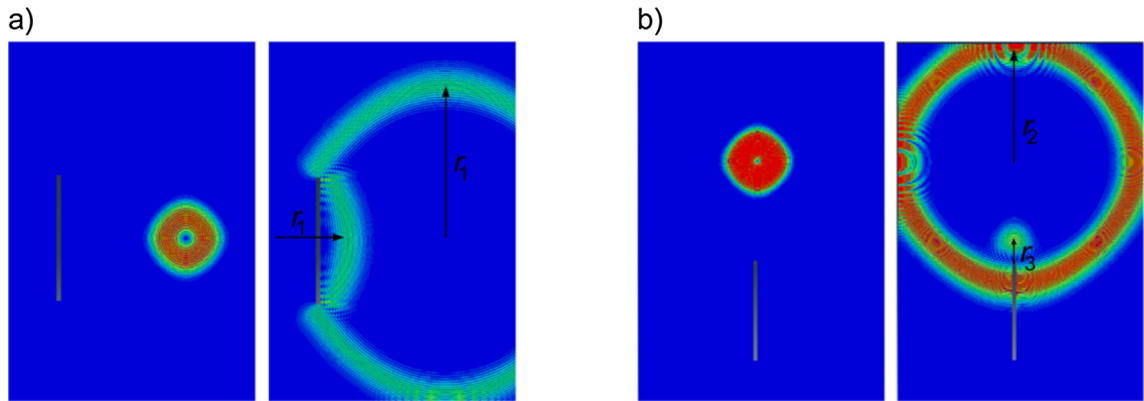
Fig. 3. Wave reflection from a) middle part of the crack, b) end point of the crack (material parameters of the steel: E = 213 GPa, v = 0.33, ρ = 7780 kg/m^3).
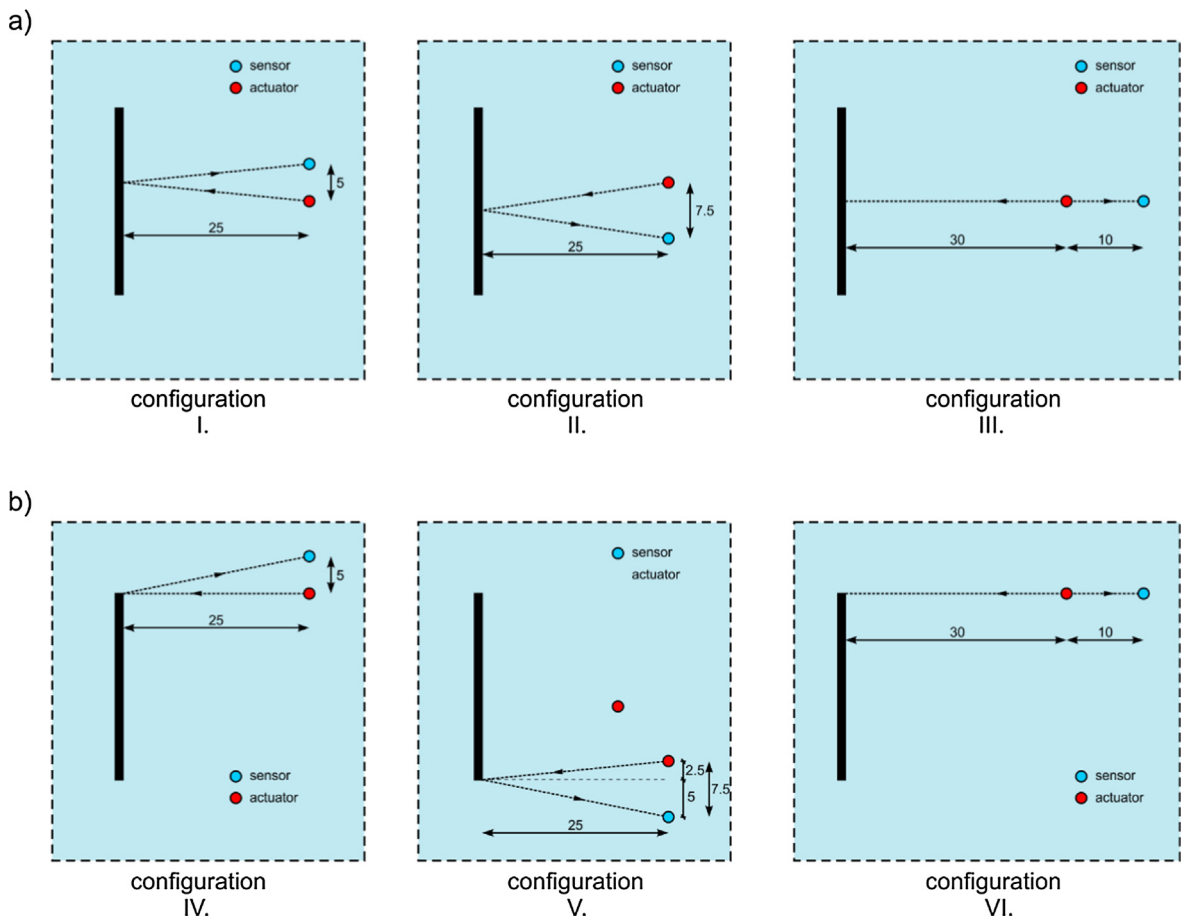

Fig. 4. Configurations of the actuator-sensor pair registering a) reflections from the middle point of the crack, b) reflections from the end point of the crack.

In the registered signals both the incident wave and the reflection from the damage were identified. Because the distance between actuator and sensor was known in each case, the value of the amplitude of incident wave could be easily determined on the basis of the distance-amplitude curve traced in the previous Section 2.3 (see Fig. 2). Each signal was scaled so that the incident wave amplitude A was consistent with the expected value A_{nor} obtained on the basis of DCM (Fig. 5). Next, after the signal scaling, the normalized amplitude value of wave reflected from the crack A_{nor}^{d}, was determined and summarized in Table 1.
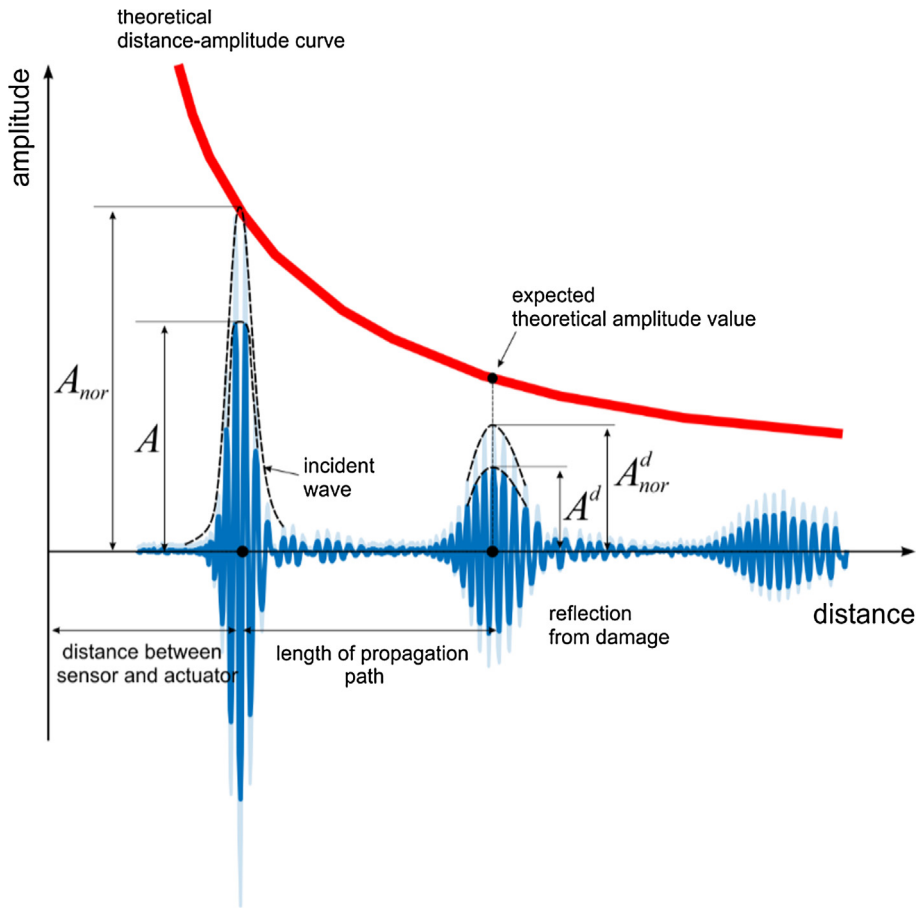
Fig. 5. The scheme illustrating the procedure of determining of the expected amplitude of the wave reflected from the crack on the basis of DCM.

Table 1
Wave interaction with the crack: comparison of the theoretical and experimental amplitudes of waves reflected from the middle and end points of the crack.

Configuration	Amplitude of incident wave		Amplitude of reflection from crack		Length of propagation path L [m]	Expected value of amplitude of reflection from crack A_t^d	Relative error [%] $\left|\frac{A_{nor}^d - A_t^d}{A_{nor}^d}\right| \cdot 100\%$
	A	A_{nor}	A^d	A_{nor}^d			
I	11.7221	0.4391	2.7822	0.1042	0.5024	0.0866	16.91
II	10.3387	0.3566	3.0200	0.1042	0.5056	0.0860	17.46
III	10.3673	0.3053	2.6868	0.0791	0.4000	0.1098	38.77
IV	8.7057	0.4391	0.3558	0.0179	0.5050	0.0861	379.79
V	11.2699	0.3566	1.0611	0.0336	0.5062	0.0859	155.75
VI	10.7483	0.3053	1.1616	0.0330	0.4000	0.1098	232.77

The lengths of the propagation paths L were known and the expected, theoretical values of the reflections' amplitudes A_t^d could be easily calculated on the basis of the analytical curve. Next, the analytical amplitudes were compared with experimentally obtained values by calculating the relative error. We can see that in the case of wave reflected from the middle part of the crack, the experimental and analytical values are consistent. The relative error does not exceed 40%. This error value could be considered large, however in comparison with errors registered for the other three cases it is not significant. In the case of reflections from the end point of the crack the analytical values determined on the basis of the propagation paths' lengths are much higher than experimental ones. The smallest error in this case was as much as 155.75%. These results showed that not only the distance but also the damage zone, where wave reflects influences on wave reflection energy. The wave is more dissipated when it reflects from the end point of the crack. This information allow for distinguishing and identifying the reflections from smooth, regular edges (e.g. edges of the plate or middle parts of the line cracks) and

reflections from irregularities (e.g. end point of the crack or localized point damage). The difference between amplitudes of reflections is used in the algorithm of crack detection and its size estimation with the minimal number of the piezo transducers.

One can see that despite the fact that both sensors used in configurations IV and V register wave reflections from the end of the crack and the lengths of the propagation distances are comparable, the difference between relative errors is significant (379.79% and 155.75%). In general, the particular configurations differ not only in the travelled distance, the point (middle or end point), where wave reflects but also the angle of reflection. Tua [5] showed that the angle of reflection has a great impact on reflection amplitude, which was not considered in this study, however it could be the source of the difference between relative errors.

3. Algorithm of reflection coefficient estimation

The relation between wave amplitude and the travelled distance allows for defining the new algorithm of line crack detection and its size estimation. The crack detection can be made with any number of sensors, however the minimal number is three. The following stages of the investigation can be distinguished:

1. *Tracing the distance-amplitude curve*. This stage requires the determination of the structural damping coefficient ξ. To this end, the ratio of at least two amplitudes recorded at different distances from the excitation source should be determined. A larger number of measurements increases the accuracy of the theoretical curve. The procedure of curve tracing was in detailed presented in Section 2.3.

2. *Selecting the transducers' configuration*. At this step actuator and at least three sensors are attached at chosen points of the investigated specimen. The straight line distances sensor - actuator denoted as $d_1, d_2.., d_N$ for each of N sensors are measured.

3. *Wave excitation and signal registration*. After wave excitation the ToF of the incident waves $t_1, t_2.., t_N$ are determined. In the presented study to estimate the ToF, the a cross-correlation between the input and the put signal was exploited. Next, for the know ToFs and distances (compare Stage 3), the group velocity for each sensor-actuator pair i $c_{gi} = d_i/t_i$ and average wave propagation velocity $c_g = (c_{g1} + c_{g2} + ... + c_{gN})/N$ are determined, respectively.

4. *Signal normalization*. The incident waves are identified and the amplitudes of their envelopes denoted as $A_1, A_2.., A_N$ are extracted. Then, the signals are scaled so that these values are consistent with theoretical values as $A_{nor,1}, A_{nor,2}.., A_{nor,N}$ determined theoretically based on the curve. The procedure of signal normalization is presented in Fig. 5.

5. *Extracting the information about waves reflected from the crack*. The fifth step is identifying reflections from the damage. Next, the amplitudes after normalization $(A^d_{nor,1}, A^d_{nor,2}.., A^d_{nor,N})$ and the ToFs $(t^d_1, t^d_2.., t^d_N)$ are extracted.

Comparison the theoretical and experimental results. On the basis of the ToFs and wave velocity c_g, the lengths of the propagations paths $L_1, L_2 \ldots, L_N$ are calculated:

$$L_i = c_g t^d_i. \tag{10}$$

For the experimental lengths of the traveled distances, the theoretical amplitudes of reflections $A^d_{t,1}, A^d_{t,2}.., A^d_{t,N}$ are designated using distance-amplitude curve. If the experimental and theoretical results are consistent, it can be concluded that the wave was reflected from a smooth surface, e.g. middle part of the crack. When the results are very divergent, significant energy dissipation occurred during the reflection, it allows to conclude that wave was reflected from the end of the crack. An unambiguous determination of whether the wave was reflected from the edge or the end of the crack allows for the more accurate estimation of the damage length. This stage of the algorithm can be also realized in a different way. Instead of comparing the amplitudes, we can compare the theoretical and experimental propagation paths' lengths. On the basis of the reflection amplitude the corresponding propagation path length can be determined and compared with experimental result calculated based on the ToF. The comparison of the amplitudes is shown in the Section 2.4 of this paper (see Table 1). In the following parts of the article we present a comparative analysis of the propagation paths' lengths.

7. *Creating the damage map*. The final step is to determine the location, orientation and size of the crack. Damage detection algorithms for metallic plates have been already extensively described in many previous works e.g. [6,14]. In the standard approach, each actuator-sensor pair is considered as two focal points of an ellipse, while the determined length of the propagation path is equal to the doubled semi-major axis. In the case of the point damage, its location can be indicated by the identifying the intersection point of the ellipses. When the line-crack is considered, its ends points are indicated by intersection points of ellipses, while crack orientation is determined by tangents to the ellipses [14].

The main advantage of the above seven-step algorithm is that only three sensors (two sensors detecting both crack's end points and one for tracing the tangent and determining the orientation of the crack) are required, which so far was the required minimum number of sensors for the point damage detection. The main disadvantage of the proposed approach is the need for the reference measurements that are used to determine the theoretical distance-amplitude curve. The correctness and usefulness of the described algorithm in the crack detection and its size estimation is verified in the further chapter of the paper.

4. Experimental investigation

4.1. Plate model

The experimental investigations were conducted on the model of the steel plate with dimensions of 125 cm × 125 cm and a thickness of 0.1 cm and it was made of the same steel as previously investigated specimens (compare Section 2.3: E = 213 GPa, v = 0.33, ρ = 7780 kg/m^3) The damage in the form of line crack was cut through the plate thickness on the rectangular area. The width of the notch was 1 cm while its length was 25 cm. The geometry and photographs of the damage are shown in Fig. 6.

The excitation and the measurements of elastic waves were carried out by the device PAQ-16000D and piezoelectric transducers Noliac NAC2002. As previously, the Lamb wave excitation was realized in the form of a wave packet consisting of five-cycle sine modulated by a Hann window with the carrier frequency equal 100 kHz and the input voltage was 10 V. The excitation frequency and the number of cycles were chosen on the basis of the multi-criteria analysis including the time duration of the wave packet, group velocity, spreading the wave packet because of the dispersion effect and the signal readability.

4.2. Configurations of the transducers

In general, four main scenarios may occur during the experimental investigation (Fig. 7). The first scenario assumes that two sensors register the reflections from the particular end points of the crack, while the third sensor captures the reflection from the middle part of the damage. In the second scenario only one sensor registers reflection from the one end of the crack (or two sensors register reflections from the same end) and two other sensors register reflections from the middle part. The second end point remains undetected. The third scenario is analogous to the second one, but this time the wave reflects from the second end point of the crack. The last scenario assumes that all sensors register only reflections from the middle part of the crack and no reflections from the crack end points are captured this time. To realize all scenarios, verify the correctness of the theoretical predictions and test the effectiveness of the novel crack detection algorithm, four different configurations of the four piezo transducers presented in Fig. 7 were used at this stage of the experiment. One transducer acted as an actuator (A), while three others (S1, S2 and S3) registered wave propagation signals. The shortest wave paths were plotted to indicate places, where wave is expected to reach and reflect first.

4.3. Results of the experimental crack detection

In the following step, waves were subsequently excited and signals registered were processed according to the algorithm described in the Chapter 3. The exemplary time domain signals registered for configuration #1 are presented in Fig. 8. The piezoelectric transducers clearly acquired the wave interaction with the damage and the identified reflections were highlighted. In the signal presented in Fig. 8b the additional low-amplitude symmetric mode was identified. However, as mentioned above, because the excitation was perpendicular, only antisymmetric modes were taken into account in the further investigations. Their average wave group velocity c_g calculated according to the 3rd algorithm step was 1837.67 m/s. The
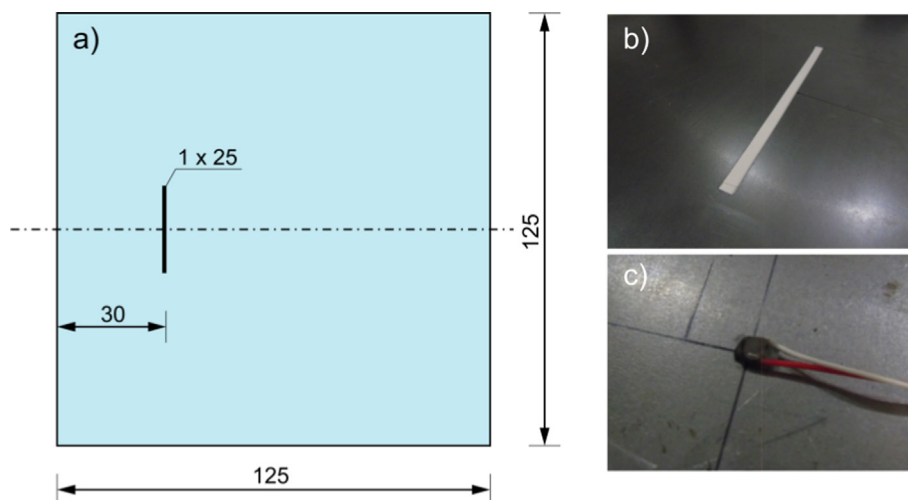
Fig. 6. Geometry of the investigated plate-like structures: a) plate with line crack and b) the photographs of the damage, c) transducer attached on the plate surface.
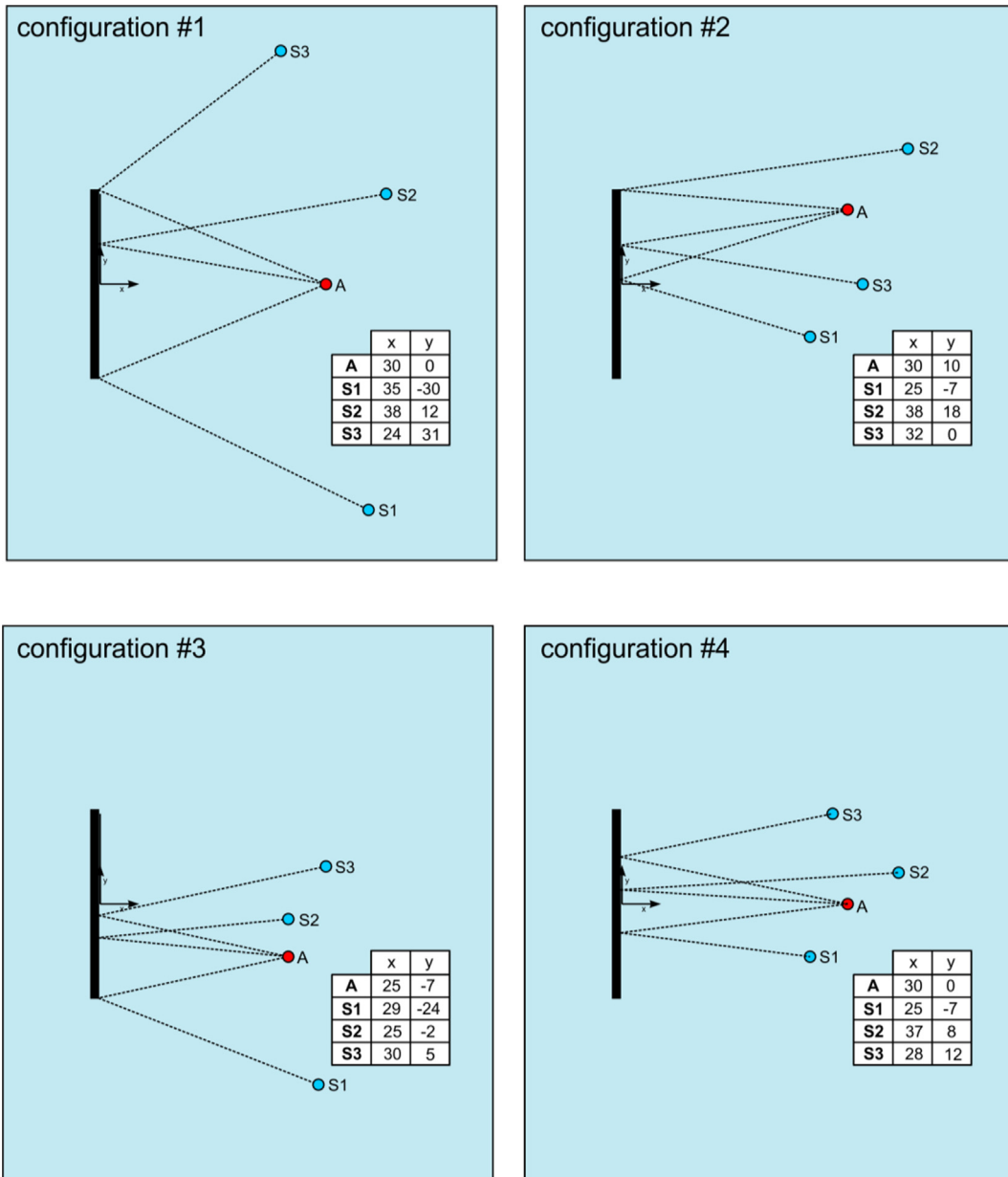
Fig. 7. Configurations of transducers used in crack detection procedure.

partial results for the configuration #1 obtained according to 4-6th steps (Fig. 7) i.e. ToF, length of the propagation path L, normalized amplitudes A_{nor} and A_{nor}^d and length L^t determined using theoretical distance-amplitude curve are summarized in Table 2. One can see, that the differences between experimental and analytical lengths of the propagation paths are significant in two cases (for sensor S1 and S3) and exceed several tens of centimeters. In both cases the path length obtained using amplitude is much longer than the length determined on the basis of the ToF. The strong energy dissipation and significant amplitude decrease suggest the reflection from the crack end point.

In the case of sensor S2 the absolute error is insignificant, which indicates negligible wave dissipation due to the reflection from a middle part of the crack. After identification the types of the reflections, the damage map can be created (Fig. 9). The damage maps were created in MATLAB environment using the ellipse-based binary damage imaging algorithm described in [14]. Ellipses denoted as 1,2 and 3 were plotted on the basis of the ToF obtained for sensors S1, S2 and S3, respectively. We know that the crack ends lie on ellipses 1 and 3 and the crack lies on the tangent to ellipse 2. To estimate the damage size, the tangent to ellipse 2, which crosses the ellipses 1 and 3 was traced. The length of the crack determined was 21.94 cm, while
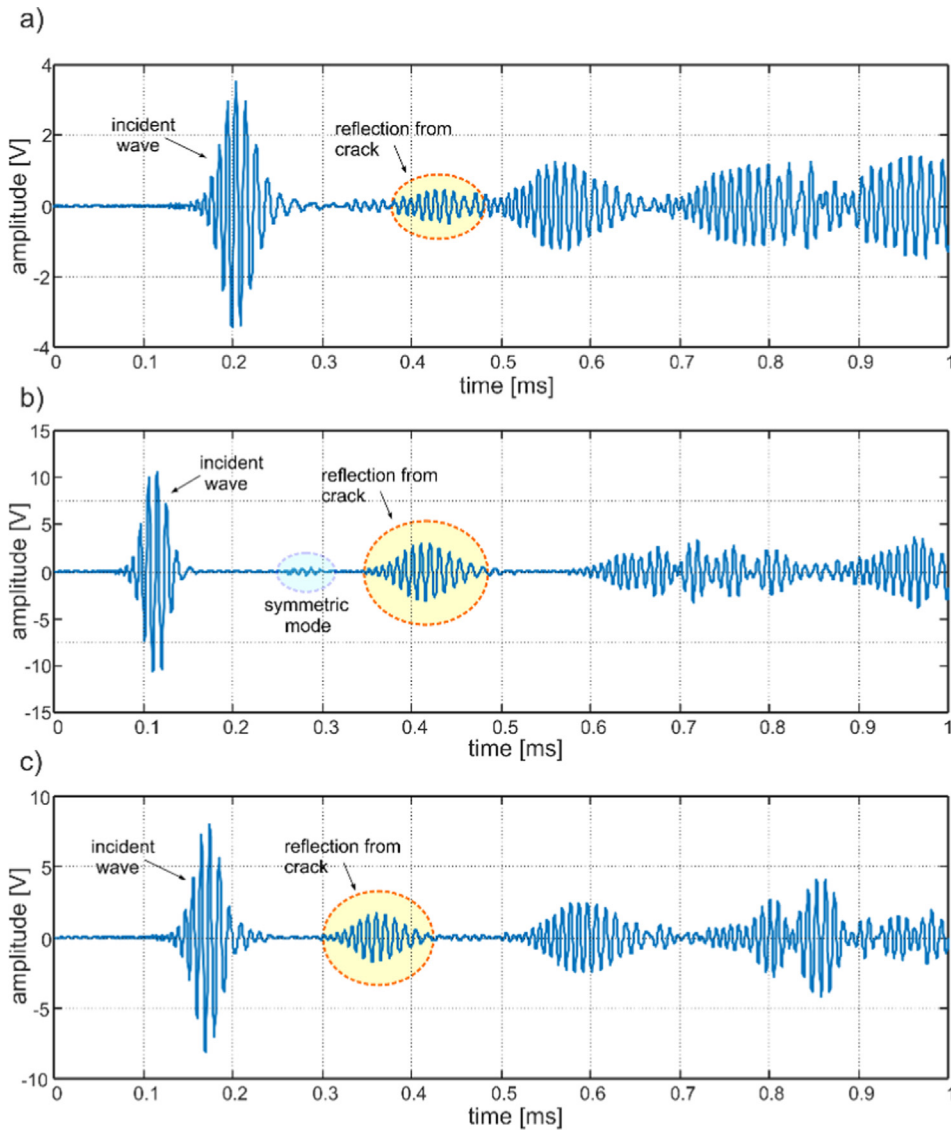
Fig. 8. Time-domain propagation signals registered for 1st transducers configuration.

Table 2
Linear crack detection in steel plate – results for configuration #1.

| Sensor	ToF [ms]	Length of the propagation path L [cm]	Normalized amplitude of the incident wave A_{nor} [-]	Normalized amplitude of the reflected wave A_{nor}^d [-]	Length of the propagation path determined on the basis of amplitude L^t [cm]	Absolute error $\lvert L - L^t \rvert$ [cm]	Remark
S1	0.400	73.52	0.1429	0.0199	158.34	84.42	Reflection from end point of crack
S2	0.372	68.33	0.2469	0.0622	67.21	1.12	Reflection from middle point of crack
S3	0.322	59.24	0.1381	0.0288	122.71	63.47	Reflection from end point of crack
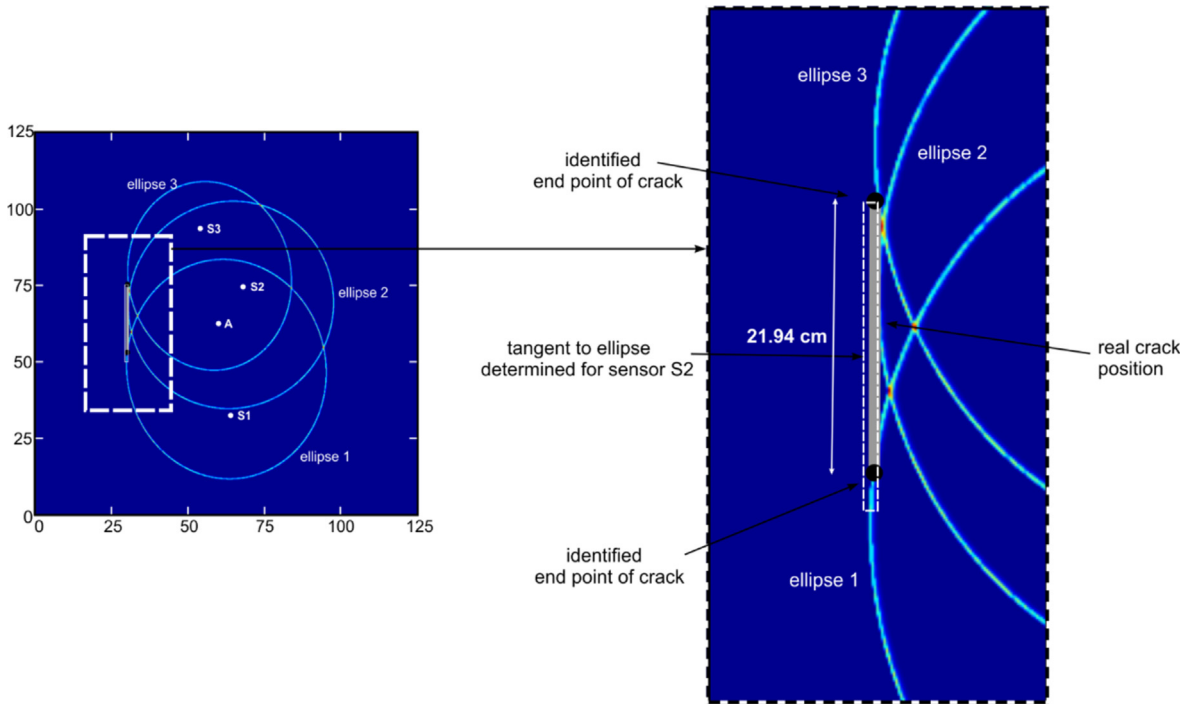
Fig. 9. Damage map created for the configuration #1.

the exact length was 25 cm. It can be seen that both damage size and its location were successfully specified based on data extracted from the only three signals.

The results for the other configurations were processed in the same way. For the configuration #2 (Table 3) the difference between distances calculated for sensor S2 can be considered as significant and for this reason one can expect that this sensor registered the reflection from the end point. In this case the crack orientation is determined by the tangent to both ellipses 1 and 3. The only detected end point is an intersection of the tangent with the ellipse 2 (Fig. 10).

The results obtained indicate unambiguously the crack orientation, which coincides perfectly with the exact actual orientation. The distance between the end point and the extreme contact point is 11.35 cm. Therefore, it can be concluded that the length of the crack is certainly >11.35 cm, however the following configuration does not allow for the exact evaluation of the damage size (Fig. 11).

The analogous results were obtained for the configuration #3 (Table 4). Based on the significant difference between the propagation paths obtained for sensor S1 and the high agreement of the analytical and experimental results for sensors S2 and S3, one can conclude that the only detected end point lies on the ellipse 1, while the crack lies on the tangent to ellipses 2 and 3. The distance between the end point and the extreme contact point is 13.7 cm. Because the second end point was not detected, the crack is assessed to be longer than 13.7 cm.

Table 3
Linear crack detection in steel plate – results for configuration #2.

| Sensor	ToF [ms]	Length of the propagation path L [cm]	Normalized amplitude of the incident wave A_{nor} [-]	Normalized amplitude of the reflected wave A_{nor}^d [-]	Length of the propagation path determined on the basis of amplitude L^t [cm]	Absolute error $\lvert L - L^t \rvert$ [cm]	Remark
S1	0.32	58.80	0.2165	0.0852	51	7.8	Reflection from middle point of crack
S2	0.379	69.73	0.2852	0.0288	122.58	52.85	Reflection from end point of crack
S3	0.348	63.91	0.3022	0.0907	48.004	15.88	Reflection from middle point of crack
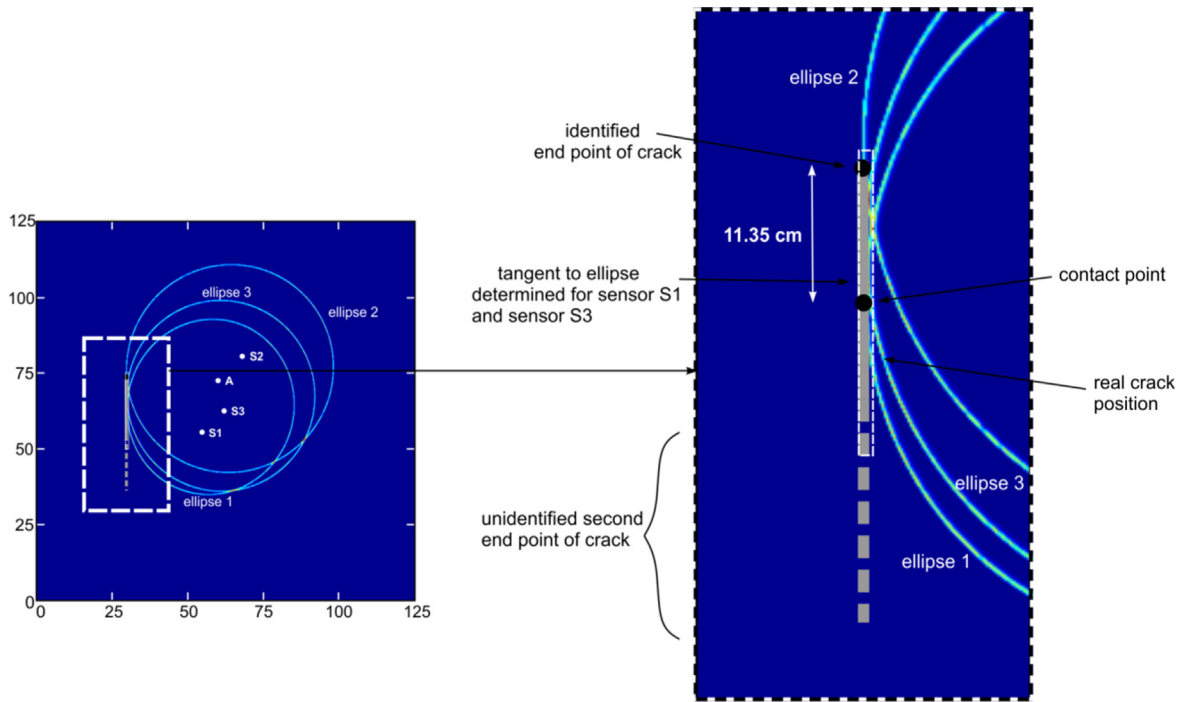
Fig. 10. Damage map created for the configuration #2.
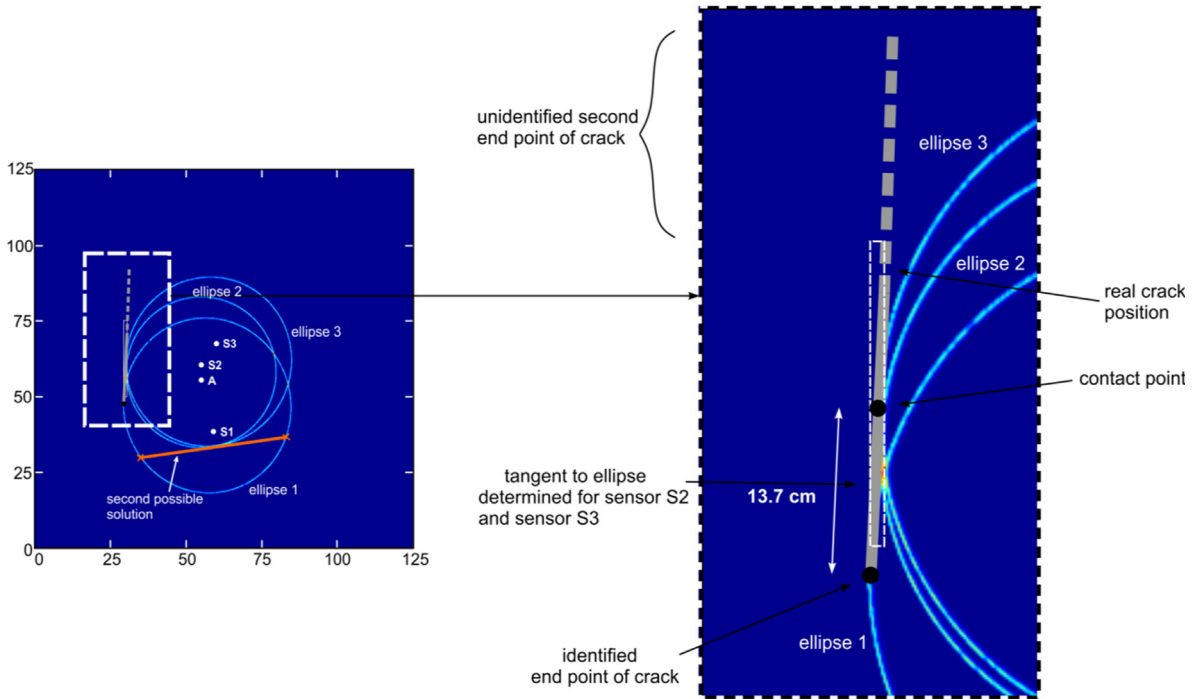

Fig. 11. Damage map created for the configuration #3.

However, one can see that in this case there are two possible solutions. One of them coincides with the exact damage position and the detected end point lies closely to actual crack end point. As the part of the second solution, the orientation and the two possible locations of the end point were indicated. The used sensors configuration is extremely unfavorable, because in this case neither the damage size nor its location can be clearly determined.

Table 4
Linear crack detection in steel plate – results for configuration #3.

Sensor	ToF [ms]	Length of the propagation path L [cm]	Normalized amplitude of the incident wave A_{nor} [-]	Normalized amplitude of the reflected wave A_{nor}^d [-]	Length of the propagation path determined on the basis of amplitude L^t [cm]	Absolute error $|L - L^t|$ [cm]	Remark
S1	0.318	58.36	0.2186	0.0174	172.94	114.58	Reflection from end point of crack
S2	0.272	49.90	0.4391	0.0725	58.89	8.99	Reflection from middle point of crack
S3	0.305	56.12	0.2629	0.0780	55.20	0.93	Reflection from middle point of crack

The results for the configuration #4 are given in Table 5. The lengths of the propagation paths calculated in two different ways differ by less than 10 cm, which means that in all cases wave was reflected from the middle part of the crack. The crack orientation can be determined by tracing the tangent to all ellipses (Fig. 12). The orientation determined perfectly reflects the actual damage location and orientation, however lack of the information about end points makes it impossible to estimate

Table 5
Linear crack detection in steel plate – results for configuration #4.

| Sensor	ToF [ms]	Length of the propagation path L [cm]	Normalized amplitude of the incident wave A_{nor} [-]	Normalized amplitude of the reflected wave A_{nor}^d [-]	Length of the propagation path determined on the basis of amplitude L^t [cm]	Absolute error $|L - L^t|$ [cm]	Remark
S1	0.301	55.28	0.3316	0.0748	57.21	1.94	Reflection from middle point of crack
S2	0.360	66.21	0.2954	0.0713	59.79	6.41	Reflection from middle point of crack
S3	0.321	58.98	0.2672	0.0888	49.01	9.97	Reflection from middle point of crack
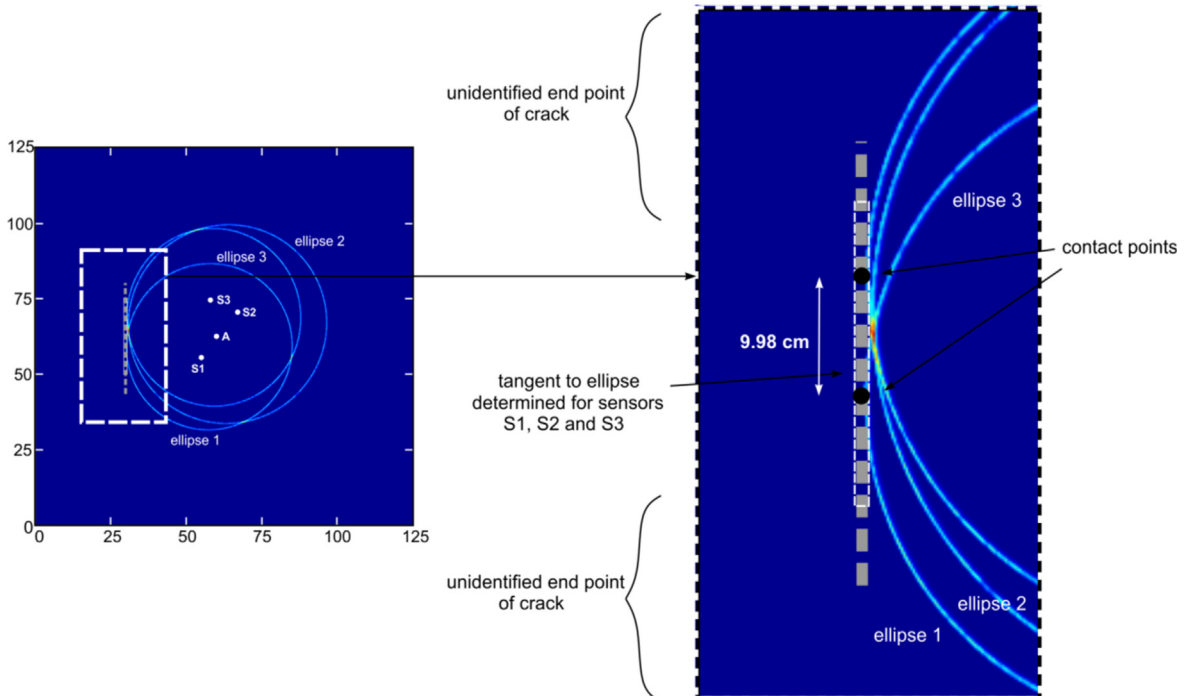
Fig. 12. Damage map created for the configuration #4.

the damage size. The only thing we can conclude is that the crack is longer than the distance between extreme contact points (9.98 cm).

5. Discussion

The experimental data acquired for four different configurations of piezoelectric transducers showed that developed crack detection algorithm can be efficiently employed in both location and the size assessment of the damage. We have shown that based on the amplitude value it is possible to indicate which wave packet was reflected from middle or end points of the crack. On the basis of the results obtained we can conclude that the error threshold that aided the qualification whether the wave reflects from the middle or end part of the damage is equal to 50%. When the error was higher than 50%, the wave reflected from the end of the crack and otherwise, wave reflected from the middle part. In all cases the recognition of the reflection type performed using the proposed algorithm agreed with the theoretical predictions made on the basis of Fermat's principle and the shortest propagation paths (compare Tables 2–5 and Fig. 7). The main aim was to develop the algorithm of line crack detection and its size estimation using the minimal number of sensors. In the presented study the damage maps were created using the data collected by three sensors, which so far was the minimal number to detect and localize only the point damage. Despite the promising results, the conclusions, which must be taken into account in the case of the further practical application of the projected solution, must be formulated.

The first aspect to consider is the critical damage size that can be detected using presented approach. The crack considered in the paper is characterized by the relative significant width (1 cm). However, the width of the damage has no influence on the results. Thus, the algorithm can be efficiently used is detection of narrower notch cracks. The damage length can also be considered significant (25 cm) compared to wavelength (1.84 cm). In general, the wavelength should not be longer than length of detected damage. The higher the frequency, the shorter the wavelength, but also the higher number of possible wave modes, which can be excited. The application of higher frequencies allows for detection of smaller damages, but also entails possible difficulties in signals interpretation.

The experimental studies included four different configurations of piezoelectric transducers. In each case the transducers configuration was designed to realize different damage detection scenarios. While the detection of the line crack was possible in each case, its size assessment could be made only using an appropriate configuration of sensors. The configuration #1 allowed for both crack detection and size assessment. The results presented in this section fully confirmed the correctness and effectiveness of the novel procedure of line crack detection. The damage size has been estimated with good accuracy. The other configurations were designed to show the limitations of the proposed algorithm. The configurations #2 and #3 allowed for detection only the orientation and one end point of the crack. Moreover, in the case of configuration #3 two solutions were possible. The last case concerned the situation, when only the orientation of the crack can be detected. In the paper [14] was shown that for a given configuration of sensors, regardless their number, there exist a certain limit length of the crack, which can be detected. The limit length depends on extreme transducers' positions. In general, the more scattered the sensors are, the longer crack can be efficiently detected. Note that in the cases of configurations #2, #3 and #4 sensors lie much closer together than in the case of configuration #1. Using the formulae given in paper [14] the limit detectable crack lengths for particular sensors configurations considered in the previous chapter were calculated, summarized and compared with experimentally determined crack lengths (Table 6).

In three cases the detectable limit crack length was significantly shorter than 25 cm, which indicates that detecting the extent of the whole crack and estimating its size was impossible because of the unfavourable transducers' positions, but not because of the applied damage detection procedure. An application of the developed algorithm allowed to unequivocal statement that the length of the crack is greater than the length determined in experimental tests. In such a case, when at least one end point was not detected the transducers configuration must be re-designed. From the point of view of detection of long cracks or long lasting monitoring of damage development, it is advantageous to arrange the sensors as far from each other as possible. From the other hand, too large spacing between the sensors can lead to registration the reflections from the edges of the plate, which can significantly hinders the signals interpretation.

5.1. Monitoring of the damage development

The developed procedure of the recognizing the reflections types has a great potential for long lasting monitoring of the damage propagation. It allows to state if the crack propagates or its size remains the same. The potential application of the

Table 6
Comparison of the limit detectable lengths with damage size obtained experimentally.

Configuration	Detectable limit crack length [cm]	Damage size assessment based on proposed algorithm [cm]
#1	31.07	21.94
#2	12.80	>11.35
#3	13.32	>13.7
#4	10.28	>9.98

described algorithm is discussed on the example shown in Fig. 13. At an early stage of the damage development, when it is point-like (*Stage I*) all sensors register the reflections characterized by the lower amplitude, than determined on the basis of the theoretical distance-amplitude curve. When the crack propagates (*Stage II*), the lengths of the propagation paths change and, in consequence, the changes in ToFs are observed. Moreover, some sensors may capture the waves bounced from the middle part of the crack, which would result in an increase of the reflections' amplitudes. The further damage development manifests only by changes in the ToFs determined for the waves reflected from the end points (*Stage III*). The changes of the ToF are observed until the damage reaches the detectable length (*Stage IV*). The moment when the damage reaches the limit detectable length is manifested by no change in the ToF and the significant increase of the reflection amplitude registered for the extreme sensor, which so far captured reflection from the end point. It means that the detectable damage length is shorter than actual damage length and the configuration must be re-designed.

5.2. Other damage scenarios

In this part of the work we present the damage scenarios, which were not considered experimentally. Obviously, the number of possible damage scenarios is much larger, however three representative cases are considered here to highlight the possible difficulties, which can occur in the case of practical application. The first case concerns the situation when the damage propagates in the direction, which prevents the observation of its development and estimating the size. An inappropriate transducers configuration, even comprising a large number of sensors, allows only to detect one end point of the crack, which in turn may lead to the erroneous conclusion that detected damage is point-like (Fig. 14).

The second case is damage characterized by an large area (Fig. 15). In such a case the use of three sensors allows only for estimation the one dimension of the damage (Fig. 15a). To determine the other damage dimensions, the set of the transducers must be enriched by the additional actuator-sensor pairs (Fig. 15b).

The last discussed case is a mix-mode crack. The use of the network of three sensors provides only a rough estimation the damage size (Fig. 16a), but still the algorithm provides the possibility of diversification of reflections from the middle parts or the edges and end points of the crack. The full reconstruction of the irregular crack shape is possible only by the extending the transducers network (Fig. 16b).
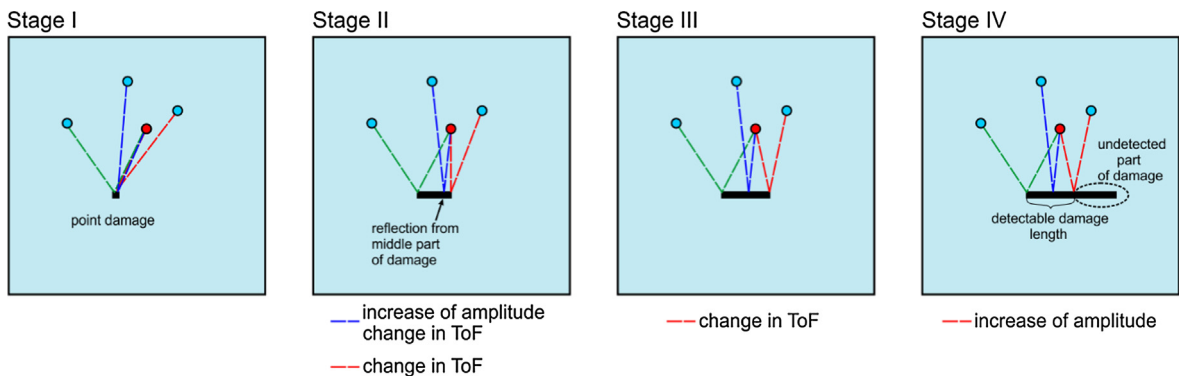

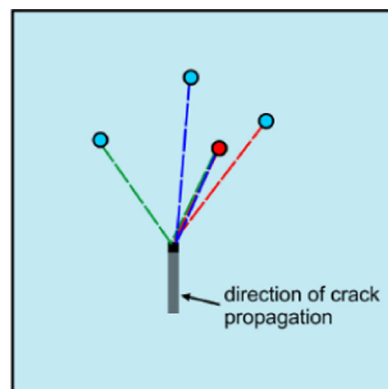**Fig. 13.** Stages of the monitoring of damage development.

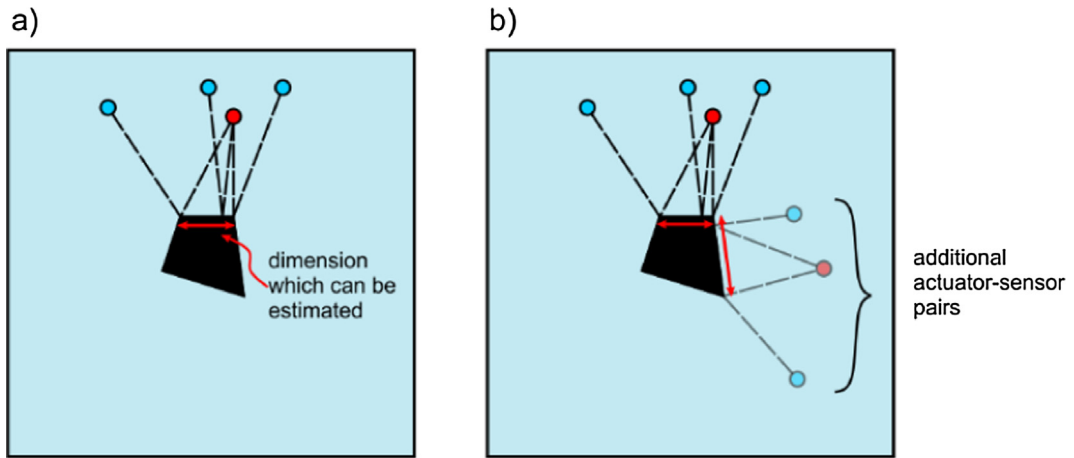**Fig. 14.** Detection of unfavorably oriented crack.

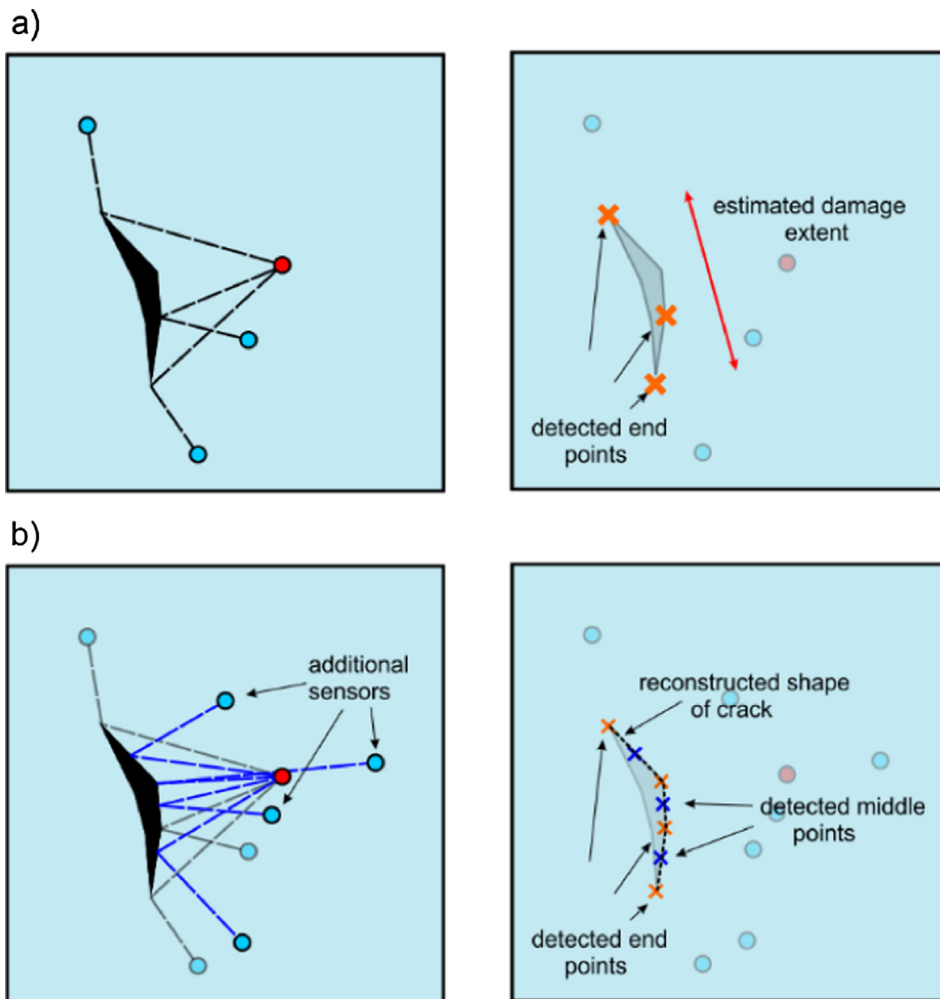**Fig. 15.** Detection and dimensions estimation of the large-size damage.

Fig. 16. Detection of the mix-mode crack: a) rough estimation of the damage extent, b) reconstruction of the damage shape with wide sensors' network.

6. Conclusions

In this paper the crack detection in plate structures using guided wave propagation was discussed. In the first step the Dispersion Compensation Method was involved to determine the analytical relation between length of the propagation path and the amplitude of the propagating wave. The correctness of the derived formula was proven during experimental investigations. On the basis of the distance-amplitude curve we have shown that wave reflecting from different parts of the damage is dissipated to varying degrees. Namely, the wave reflected from the middle crack part is less dissipated and thus is characterized by the higher amplitude than wave reflected from the end points of the crack. The difference between the particular types of the reflections allowed for formulating the algorithm dedicated to detection and size estimation of the line cracks. The effectiveness and the potential application of the developed procedure was verified during the four-stage experiment. At each stage we tested the algorithm diagnostic abilities by using different sensors' configurations. Each reflection was identified correctly, which demonstrated the correctness of the assumption about varying wave energy dissipation observed for reflections from the middle and end points. The configurations of the transducers were designed to present also the limitations of the proposed approach. Despite the fact that the developed algorithm allows to estimate the damage size with the high accuracy, this is not possible in every case. Regardless of the algorithm's efficiency, it is also necessary to use the appropriately designed sensor configuration. In the three considered cases, the sensors were too close together to capture the whole damage, which was 25 cm long.

The orientation of the crack was determined correctly in each case. Moreover, the great potential of application the algorithm in long lasting crack development monitoring was presented. The last part of the paper was devoted to discussion of application the algorithm in detection of damage characterized by different shape and size. Despite the fact that the developed method was dedicated to assessment of the line cracks damage, it was demonstrated that it can be also used in estimating the size of other damage types. It is also possible to reconstruct the shape of mix-mode damages, however the extended sensors network is required.

CRediT authorship contribution statement

Beata Zima: Conceptualization, Methodology, Software, Visualization, Investigation, Data curation, Writing - original draft, Resources, Writing - review & editing. **Rafał Kędra:** Conceptualization, Methodology, Software, Investigation, Data curation, Resources, Writing - review & editing.

Declaration of Competing Interest

The authors declare that they have no known competing financial interests or personal relationships that could have appeared to influence the work reported in this paper.

References

[1] J.L. Rose, Ultrasonic guided waves in structural health monitoring, Key Eng. Mater. 270–273 (2004) 14–21.
[2] Z. Su et al, Guided Lamb waves for identification of damage in composite structures: a review, J. Sound Vib. 295 (2006) 753–780.
[3] A. Raghavan, C.E.S. Cesnik, Review of guided wave structural health monitoring, Shock vibration, Digest 39 (2) (2007) 91–114.
[4] M. Mitra, S. Gopalakrishnan, Guided wave based structural health monitoring: a review, Smart Mater. Struct. 25 (5) (2016) 27.
[5] P.S. Tua, S.T. Quek, Q. Wang, Detection of crack in plates using piezo-actuated Lamb waves, Smart Mater. Struct. 13 (2004) 643–660.
[6] T. Wandowski, P. Malinowski, W. Ostachowicz, Damage detection with concentrated configurations of piezoelectric transducers, Smart Mater. Struct. 20 (2011) 14, 025002.
[7] M. Radzieński, Ł. Doliński, M. Krawczuk, M. Palacz, Damage localization in a stiffened plate structure using a propagating wave, Mech. Syst. Sig. Process. 39 (2013) 388–395.
[8] F. Li, H. Peng, G. Meng, Quantitative damage image construction in plate structures using a circular PZT array and lamb waves, Sens. Actuators, A 214 (2014) 66–73.
[9] P.F. Pai, H. Deng, M.J. Sundaresan, Time-frequency characterization of lamb waves for material evaluation and damage inspection of plates, Mech. Syst. Sig. Process. 62–63 (2015) 188–206.
[10] Z. Wang, P. Qiao, B. Shi, Application of soft-thresholding on the decomposed Lamb wave signals for damage detection of plate-like structures, Measurement 88 (2016) 417–427.
[11] M. Chandrashekhar, R. Ganguli, Damage assessment of composite plate structure with material and measurement uncertainty, Mech. Syst. Sig. Process. 75 (2016) 75–93.
[12] Z. Liu, K. Sun, G. Song, C. He, B. Wu, Damage localization in aluminum plate with compact rectangular phased piezoelectric transducer array, Mech. Syst. Sig. Process. 70–71 (2016) 625–636.
[13] C. Schaal, A. Mal, Lamb wave propagation in a plate with step discontinuities, Wave Motion 66 (2016) 177–189.
[14] B. Zima, M. Rucka, Guided waves for monitoring of plate structures with linear crack of variable length, Arch. Civ. Mech. Eng. 16 (3) (2016) 387–396.
[15] J. Chen, Z. Li, K. Gong, Nondestructive testing method based on lamb waves for localization and extend of damage, Acta Mech. Solida Sin. 30 (2017) 65–74.
[16] J. Jingpin, M. Xiangji, H. Cunfu, W. Bin, Nonlinear Lamb wave-mixing technique for micro-crack detection in plates, NDT&E International 85 (2017) 63–71.
[17] H. Zou, Z. Yang, C. Xu, S. Tian, X. Chen, Damage identification for plate-like structures using ultrasonic guided wave based on improved MUSIC method, Compos. Struct. 203 (2018) 164–171.
[18] H.-W. Kim, F.-G. Yuan, Enhanced damage imaging of a metallic plate using matching pursuit algorithm with multiple wavepaths, Ultrasonics 89 (2018) 84–101.
[19] P. Kudela, M. Radzieński, W. Ostachowicz, Z. Yang, Structural Health Monitoring system based on a concept of Lamb focusing by the piezoelectric array, Mech. Syst. Sig. Process. 108 (2018) 21–32.

[20] S. Cantero-Chinchilla, J. Chiachio, M. Chiachio, D. Chronopoulos, A. Jones, A robust Bayesian methodology for damage localization in plate-like structures using ultrasonic guided-waves, Mech. Syst. Sig. Process. 122 (2019) 192–205.
[21] N. Mori, S. Biwa, T. Kusaka, Damage localization method for plates based on the time reversal of the mode-converted Lamb waves, Ultrasonics 91 (2019) 19–29.
[22] D. Sen, A. Aghazadeh, A. Mousavi, S. Nagarajaiah, R. Baraniuk, Sparsity-based approaches for damage detection in plates, Mech. Syst. Sig. Process. 117 (2019) 333–346.
[23] A. Ghadami, M. Behzad, H.R. Mirdamadi, A mode conversion-based algorithm for detecting rectangular notch parameters in plates using Lamb waves, Arch. Appl. Mech. 85 (2015) 793–804.
[24] C. Ramadas, K. Balasubramaniam, A. Hood, M. Joshi, C.V. Krishnamurthy, Modelling of attenuation of Lamb waves using Rayleigh damping: Numerical and experimental studies, Compos. Struct. 93 (2011) 2020–2025.
[25] J.L. Rose, Ultrasonic waves in solid media, Cambridge University Press, 1999.
[26] Z. Su, L. Ye, Identification of Damage Using Lamb Waves, From Fundamentals to Applications. Springer-Verlag, Berlin Heidelberg, 2009.
[27] P.D. Wilcox, A rapid signal processing technique to remove the effect of dispersion from guided wave signals, IEEE Trans. Ultrason. Ferroelectr. Freq. Control 50 (2003) 419–427.
[28] K. Xu, D. Ta, P. Moilanen, W. Wang, Mode separation of Lamb waves based on dispersion compensation method, J. Acoust. Soc. Am. 131 (4) (2012) 2714–2722.
[29] H. Lamb. On waves in elastic plate. Proceedings of the Royal Society of London. Series A. London 93 (1917) 114–128.
[30] R.P. Feynman, R.B. Leighton, M. Sands, The Feynman Lectures on Physics. Volume 1. Mainly Mechanics, radiation and heat, California Institute of Technology, 1963.